ELSEVIER

Sensors and Actuators B 73 (2001) 100–105

SENSORS AND ACTUATORS B CHEMICAL

www.elsevier.nl/locate/sensorb

Physical mechanism of reflectance inversion in hydrogen gas sensor with Pd/PVDF structures

Chinhua Wang*, Andreas Mandelis, Keung Patrick Au-Ieong

Photothermal and Optoelectronic Diagnostics Laboratories, Department of Mechanical and Industrial Engineering, University of Toronto, 5 King's College Road, Toronto, Ont., Canada M5S 3G8

Received 20 June 2000; received in revised form 10 September 2000; accepted 20 September 2000

Abstract

The physical mechanism of the reflectance inversion phenomena observed in thin-film Pd on polyvinylidene fluoride (PVDF) optical hydrogen sensor structures (Pd/PVDF) upon exposure to hydrogen gas has been investigated. Based on experimental observations using sensors with or without a metallic back-surface coating, a theoretical model taking into account the infinite optical interreflections within the transparent polymer PVDF has been proposed. The understanding of the origin of the reflectance inversion is helpful in optimizing the design and performance of optical hydrogen sensors with Pd-layer active element structures. © 2001 Published by Elsevier Science B.V.

Keywords: Physical mechanism; Reflectance inversion; Pd/PVDF structure; Hydrogen sensor

1. Introduction

Hydrogen, as an important energy source, has been attracting attention as a potential energy currency in the transportation, residential, and industrial sectors. As part of the infrastructure of hydrogen-based technologies, the development of reliable and safe hydrogen-gas sensors becomes of great importance. Among a wide variety of Pd-based hydrogen detectors [1–4], all-optical monitoring of hydrogen is considered the most appropriate method owing to its inherent safe nature when compared with techniques requiring electrical contacts/measurements. Butler [5,6] reported an optical sensor that monitored the amount of light reflected from a thin palladium film at the tip of an optical fiber. It was found that the reflectance of the palladium film decreased when hydrogen gas was absorbed into the palladium, consistent with earlier reports in the literature [7]. Chadwick et al. [8] reported a hydrogen sensor based on the optical generation of surface plasmons in palladium/nickel alloys. A sharp decrease in reflected light intensity from the glass/metal interface was also observed when surface plasmons were generated. In view of the sensor structures in these two cases, both devices are of similar optical geometry, in which the incident light impinges onto the internal Pd surface through either an optical fiber or a glass prism, while the external surface of Pd coating is exposed to the ambient gas. More recently, following the introduction of Pd/PVDF photopyroelectric (PPE) sensors [9,10], as well as a modulated optical transmittance hydrogen sensor [11], a combined dual optical reflectance/interferometric PPE hydrogen sensor [12] was developed and reported. This hydrogen sensor employs a Pd/PVDF/NiAl multi-layer structure, in which both metallic coatings on the polymer base act as electrodes. In addition, the Pd coating also acts as the hydrogen sensitive membrane. An optical (usually laser) beam is incident onto the external surface of the Pd coating, while the surface is exposed to the ambient gases. In our laboratory it was found that the reflectance from the Pd coating decreases when the thin film is exposed to hydrogen gas, if the Pd coating is thick (>8 nm). This is further consistent with earlier reports [7,8] on the physical behavior of hydrogen sensors using Pd thin films. In contrast, the reflectance was unexpectedly found to *increase* after exposure of the thin film to H_2 in the case of Pd coatings thinner than 8 nm. This reflectance-inversion phenomenon in the case of ultrathin Pd coatings was also found by Kalli et al. [13]. These authors studied extremely thin Pd coatings (0.1, 0.5, and 1 nm) on Si wafer substrates. They qualitatively advanced the hypothesis that the ''anomalous'' reflectance inversion was a result of the combination effect of surface and interface among the hypothesized small Pd clusters on the Si surface [13].

In this paper, we investigate further the experimental and corresponding theoretical evidence on the mechanism of the

* Corresponding author.

0925-4005/01/$ – see front matter © 2001 Published by Elsevier Science B.V.
PII: S0925-4005(00)00661-4

foregoing reflectance inversion using three samples of the Pd/PVDF structure with various thicknesses of Pd, in the presence or absence of a back-surface NiAl coating. It is found that the back-surface coating plays a crucial role in the reflectance-inversion phenomena. Based on the experimental findings, a theoretical model is proposed based on the multiple internal optical reflections between two metallic coatings. The theoretical simulation is found to be in good agreement with the experimental results and can be used as a guide toward designing Pd/PVDF sensor devices optimized with respect to ambient hydrogen gas sensitivity.

2. Experimental and results

The experimental arrangement is shown in Fig. 1. A He-Ne laser operating at 632.8 nm was used as the optical probe. The beam was amplitude-modulated using a mechanical chopper, thereby generating a nearly-square-wave incident intensity waveform at 10 Hz. The probe beam was directed onto the Pd surface at a small incidence angle very close to the surface normal. The reflected and transmitted components of the probe beam were directed to two photodiodes (PD), the outputs of which were coupled to lock-in amplifiers whereby the demodulated dc signals were synchronously detected as the reflectance and transmittance channels, respectively. The lock-in amplifiers were interfaced to personal computers for subsequent data acquisition. For all the data presented the lock-in time constant was maintained at 1 s.

Three Pd/PVDF/NiAl thin-film samples were fabricated and studied. They had the same PVDF base of 52 μm thickness, and the same NiAl layered backing coating of 50 nm thickness (15 nm Ni + 35 nm Al) on one surface. The active surface was coated with three different thicknesses of Pd, 3.8, 6.5, and 8.0 nm, respectively, as specified by the manufacturer. The sensors were placed in a closed test cell, which allowed controlled amounts of hydrogen in balanced nitrogen (N_2) to flow over both surfaces of the devices. The test cell was made of aluminum with an inlet and an outlet for gas mixture flows, and two optical windows for the incident laser beam as well as and for the reflected and the transmitted beams. All gases were provided in gas cylinders controlled by pressure regulators for accurate mixture formation. Gas flows were monitored by suitable flow meters. High purity hydrogen (99.999%) and zero-grade nitrogen (99.9975%) from Matheson Gas Products were used to obtain the desired hydrogen concentrations and to give a homogeneous flow with flow rates of up to 880 ml/min.

Experiments were conducted according to the following protocol: for each sensor, the reflectance and the transmittance signals were first measured before and after exposure to hydrogen/nitrogen mixtures with the intact Pd/PVDF/NiAl. Then, the back-surface NiAl coating was etched away using a cotton Q-tip soaked in methyl alcohol and cleanser. The sensor was thus reduced to a two-layer (Pd/PVDF) structure, and the measurements of reflectance and transmittance in the absence and in the presence of hydrogen gas were repeated. To compare identical experimental conditions, the experiment was conducted at a hydrogen concentration of 9% for all sensors. This is an optimal concentration, taking into account the low adsorption and absorption capacity of hydrogen in very thin Pd-coatings on one hand and signal saturation at high concentrations on the other.

Fig. 2 shows the experimental reflection signal response using a Pd/PVDF/NiAl sensor with 8 nm-thick Pd at 9% hydrogen concentration in nitrogen. Due to the large optical absorption of the back-surface NiAl coating, the sample was virtually opaque, therefore, no transmittance signal was measured. The reflectance decreased after hydrogen gas was introduced, consistently with earlier results [7,8,12]. This phenomenon has been explained in terms of Fermi level rise in the Pd metal with hydrogen concentration. The hydrogen atoms in Pd act as electron donors filling empty electronic states and subsequently shifting the Fermi level

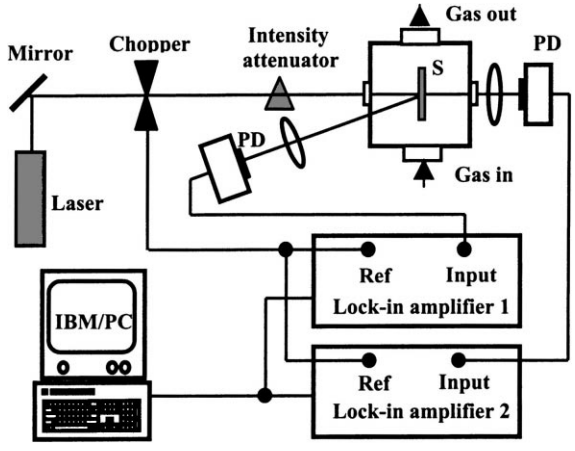

Fig. 1. Schematic representation of the Pd/PVDF/NiAl optical sensor setup. S: multi-layer sensor with Pd facing the incident laser beam; PD: photodiode.

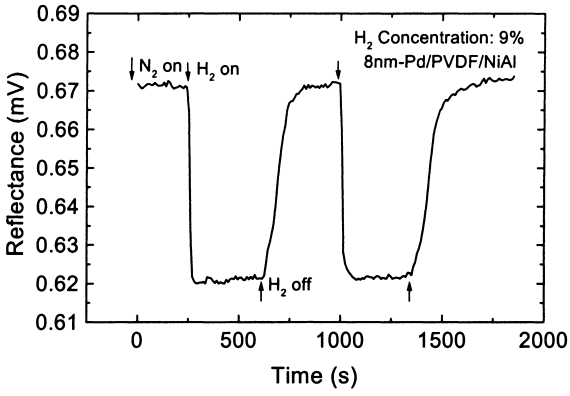

Fig. 2. Optical reflectance signal as a function of time using a 8 nm-Pd/PVDF/NiAl sensor.

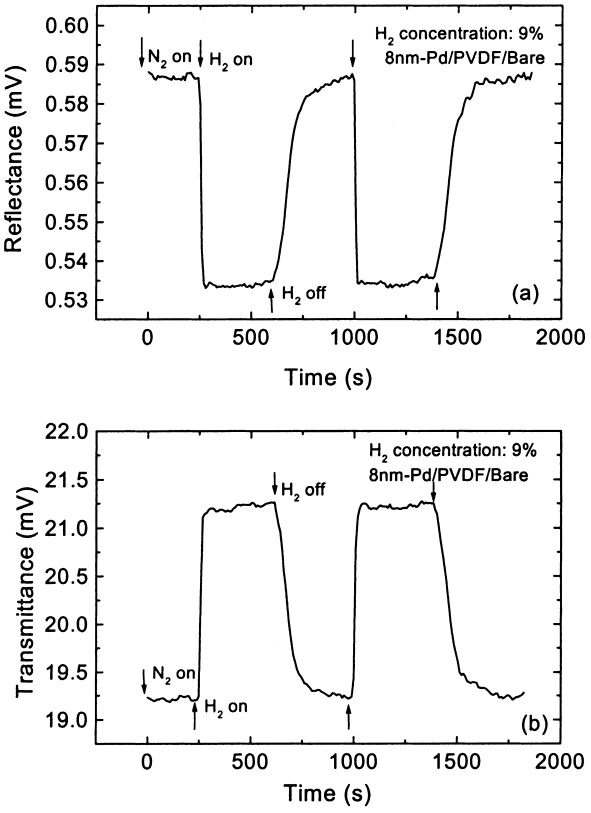

Fig. 3. Simultaneously measured optical reflectance (a) and transmittance (b) as a function of time using the same sensor as in Fig. 2, with the back-surface NiAl coating removed.

upwards, thus reducing the probability of optical transitions. This tends to render the Pd film more transparent to the incident optical radiation and enhance the optical transmittance, while depressing the reflectance. To investigate the effect of the back NiAl coating, Fig. 3(a) and (b) show the simultaneously measured reflectance and transmittance signals using the same sensor after etching of the back NiAl coating. It can been seen that the overall reflectance signal decreases from ~0.67 mV (before NiAl coating etching in Fig. 2) to ~0.59 mV (after etching away the NiAl coating) prior to the introduction of hydrogen. This is consistent with a reflectance decrease due to the absence of contributions from the back-surface NiAl metallic layer. Nevertheless, the reflectance signal decreased after the introduction of hydrogen, similar to Fig. 2. The magnitude change of the reflectance before and after exposure to hydrogen, $\Delta R \approx 0.05$ mV, is approximately the same as that in Fig. 2. In Fig. 3(b), a strong transmittance signal $\Delta T \approx 2.0$ mV is observed, which increased after the introduction of hydrogen, in a manner complementary to the reflectance behavior.

Fig. 4 shows the experimental results using the sensor with the 6.5 nm-Pd/PVDF/NiAl structure. Opposite to Fig. 2, the reflectance *increases* after the introduction of hydrogen gas. To investigate the effect of the back-surface coating, Fig. 5 shows experimental reflectance and transmittance responses using the same sensor after the NiAl coating

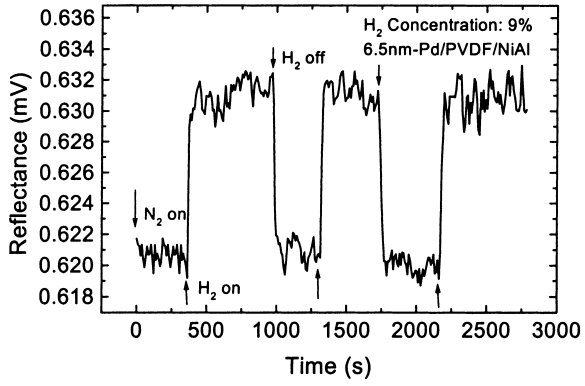

Fig. 4. Optical reflectance signal as a function of time using a 6.5 nm-Pd/PVDF/NiAl sensor.

was removed. It is seen that the reflectance signal switches direction, decreasing with increasing hydrogen concentration, in a manner similar to that of the 8 nm-Pd sensor in Fig. 3(a). Of course, the overall signal-to-noise ratio (SNR) is worse than that from the thicker Pd-coated sensor, because the hydrogen retaining capacity of the Pd film has decreased. When the transmittance signal, Fig. 5(b), is compared to that of Fig. 3(b), it is seen that the overall signal *level* is much higher in Fig. 5(b), which is reasonable due to the lower optical absorption by the thinner Pd coating. It is noted that

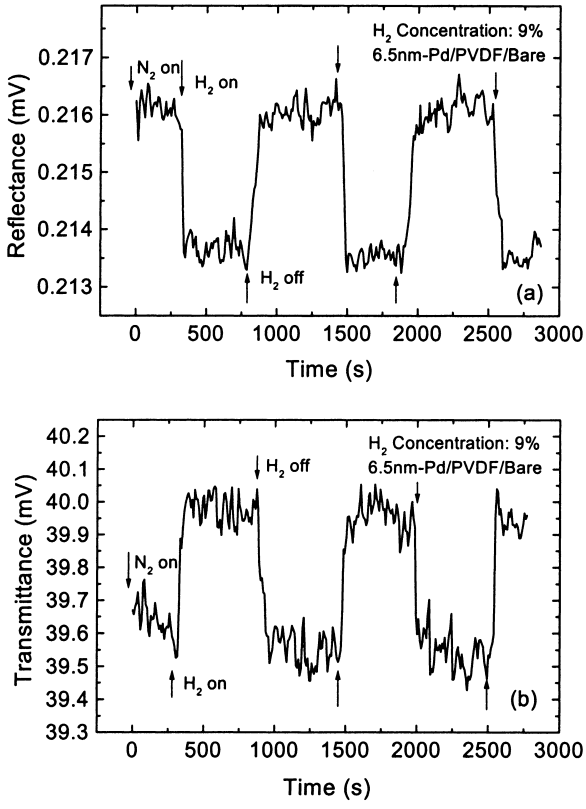

Fig. 5. Simultaneously measured optical reflectance (a) and transmittance (b) as a function of time using the same sensor as Fig. 4, with the back-surface NiAl coating removed.

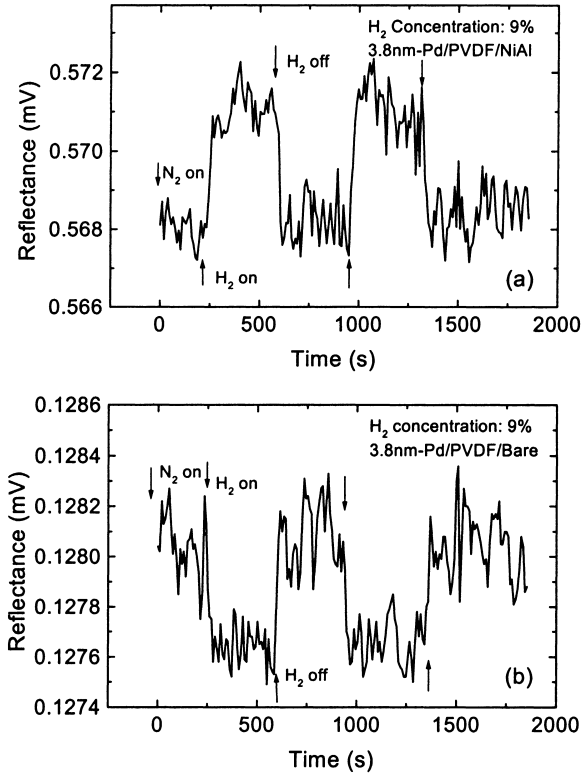

Fig. 6. Optical reflectance signal as a function of time (a) using a 3.8 nm-Pd/PVDF/NiAl sensor; and (b) using the same sensor with the back-surface NiAl coating removed.

$\Delta T \approx 0.5$ mV only for the 6.5 nm thick Pd film, compared to 2.0 mV for the 8 nm film. This trend is consistent with the fact that fewer hydrogen atoms can be absorbed by the thinner Pd film, thus resulting is smaller electronic level shifts and net changes in the optical functions R, T and A (absorptance) of the active element.

Fig. 6 shows further experimental results using the 3.8 nm-Pd/PVDF/NiAl sensor before and after removal of the NiAl coating. Once again, it is shown in Fig. 6(a) that the reflectance in the presence of the back-surface NiAl coating increases after the introduction of hydrogen, and it decreases after the NiAl coating was removed, as shown in Fig. 6(b). Here only the reflectance signals were displayed, because the transmittance change ΔT was too small to be detected after the removal of the NiAl coating due to the very large background transmittance signal baseline in the lock-in amplifier.

3. Theoretical model

The experimental results using three sensors with the same PVDF base and same thickness of back-surface NiAl coating, but different thickness of Pd coating, show different behavior before and after the removal of the NiAl coating. The reflectance signal exhibits the same decreasing behavior when the sensor is exposed to hydrogen gas in the case of 8 nm Pd. On the other hand, the reflectance of the 6.5 and 3.8 nm Pd sensors before and after the removal of NiAl coating is reversed. When the results after the removal of the back coating are compared, the reflectance signal is always found to decrease after the introduction of hydrogen, followed by an appropriate increase in the optical transmittance, irrespective of the thickness of Pd coating. This is consistent with the electronic "state-filling" model [7], which seems to be independent of the Pd layer thickness. Therefore, it follows that it is the contribution of the back-surface coating to the optical reflectance which determine the inversion phenomenon. To put this conclusion on firm theoretical grounds, Fig. 7 shows the schematic of a Pd/PVDF/NiAl structure with the incident beam and multiple internal reflections. Since the thicknesses of the Pd and NiAl coatings are very small compared to the wavelength of light, both coatings are considered to be surface layers of infinitesimal thickness with optical reflectivity R_i, absorptivity A_i and transmittivity T_i ($i = 1, 2$ represents the front and back surface, respectively). The thickness of the PVDF element is l, and the bulk optical absorption coefficient of the PVDF at the wavelength of the incident laser beam is β. Taking into account all the multiple internal reflections as shown in Fig. 7, we can obtain the *effective* reflectance and the transmittance for the three-layer structure as [14]:

$$R_{\text{eff}} = R_1 + \frac{T_1^2 R_2 \, \mathrm{e}^{-2\beta l}}{1 - R_1 R_2 \, \mathrm{e}^{-2\beta l}} \tag{1}$$

$$T_{\text{eff}} = \frac{T_1 T_2 \, \mathrm{e}^{-\beta l}}{1 - R_1 R_2 \, \mathrm{e}^{-2\beta l}} \tag{2}$$

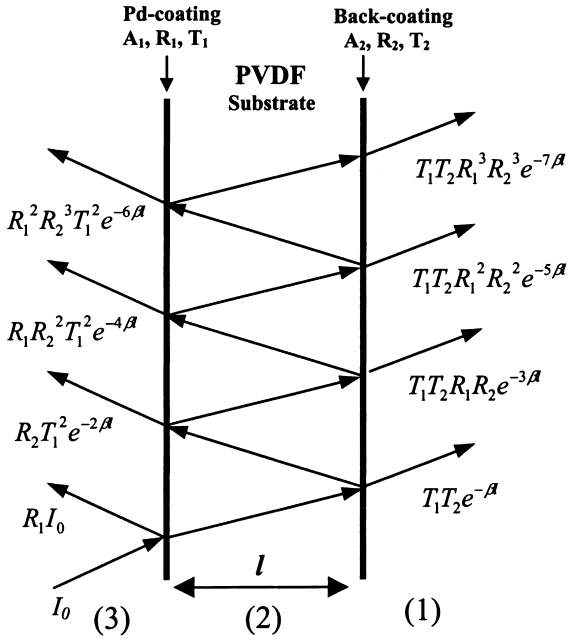

Fig. 7. Cross-section of a metal–polymer–metal structure, showing contributions of the first four internal reflections to the effective reflectance and transmittance.

It is noted that R_{eff} and T_{eff} are the quantities actually monitored as "reflectance" and "transmittance" in our experiments. The effective reflectance and transmittance are functions of the reflectivity and transmittivity of the front and back surfaces. Eqs. (1) and (2) are simplified versions of the thin film reflection and transmission equations [15]:

$$\hat{R} = \frac{\hat{r}_{32} + \hat{r}_{21}\,\mathrm{e}^{-2\mathrm{i}\hat{k}_2 l}}{1 + \hat{r}_{32}\hat{r}_{21}\,\mathrm{e}^{-2\mathrm{i}\hat{k}_2 l}} = \hat{r}_{32} + \frac{\hat{r}_{21}\hat{t}_{32}\hat{t}_{23}\,\mathrm{e}^{-2\mathrm{i}\hat{k}_2 l}}{1 - \hat{r}_{23}\hat{r}_{21}\,\mathrm{e}^{-2\mathrm{i}\hat{k}_2 l}} \tag{3}$$

and

$$\hat{T} = \frac{\hat{t}_{32}\hat{t}_{21}\,\mathrm{e}^{-\mathrm{i}\hat{k}_2 l}}{1 + \hat{r}_{32}\hat{r}_{21}\,\mathrm{e}^{-2\mathrm{i}\hat{k}_2 l}} \tag{4}$$

Here quantities with a circumflex indicate complex quantities. The subscripts (1–3) are associated with interfaces between the surface metallic layers (1, 3) and the PVDF interlayer (2), respectively. Furthermore, the various symbols represent:

$$\hat{r}_{ij} \equiv \frac{\hat{k}_i - \hat{k}_j}{\hat{k}_i - \hat{k}_j} = -\hat{r}_{ij} \quad \text{(complex reflection coefficient)} \tag{5}$$

$$\hat{t}_{ij} \equiv \frac{2\hat{k}_i}{\hat{k}_i + \hat{k}_j} = 1 + \hat{r}_{ij} \tag{6}$$

(complex transmission coefficient)

where $\hat{k}_j$ is the complex reflectance index defined as

$$\hat{k}_j = \frac{2\pi}{\lambda}(n_j - \mathrm{i}k_j) \tag{7}$$

Finally, the absorption coefficient of the PVDF layer is given in terms of the imaginary part of $\hat{k}_2$:

$$\beta(\lambda) = \frac{4\pi}{\lambda}k_2(\lambda) \tag{8}$$

Eqs. (1) and (2) are obtained using $R_{\text{eff}} = |\hat{R}|^2$ and $T_{\text{eff}} = |\hat{T}|^2$ in the incoherent limit [15]:

$$2\pi\left(\frac{\Delta\lambda}{\lambda^2}\right)n_2 l \geq 1 \tag{9}$$

which holds for PVDF thin layer thickness greater than the wavelength of the incident radiation. Here $\Delta\lambda$ is the effective wavelength range of the light. Under this incoherent condition, no interference among the various reflections is possible. Therefore,

$$|1 - \hat{r}_{23}\hat{r}_{21}\,\mathrm{e}^{-2\mathrm{i}\hat{k}_2 l}| \cong 1 - R_1 R_2\,\mathrm{e}^{-2\beta l} \tag{10}$$

where $R_1 \equiv |\hat{r}_{23}|^2$, $R_2 \equiv |\hat{r}_{21}|^2$. Further use of the definitions $T_1 \equiv |\hat{t}_{32}|^2$ and $T_2 \equiv |\hat{t}_{21}|^2$ immediately yields Eqs. (1) and (2).

Obviously, in the case where there is no back coating, i.e. $R_2 = 0$, the effective reflectance R_{eff} reduces to R_1, which is the single layer case. For non-zero reflectivity R_2 of the back coating, the effective reflectance of the layered device changes. Fig. 8 shows simulations of the effects of the reflectivity of the back-surface coating on the effective reflectance and transmittance of the sensor using Eqs. (1) and (2). In the simulation, the following parameters were used: $l = 52$ μm and $\beta = 0.05\ \mathrm{m}^{-1}$ [16]. The transmittivity of the front-surface Pd coating decreases exponentially with increasing thickness of the layer according to the Beer–Lambert law. This results in a proportional increase in the reflectivity R_1 of the front surface. Earlier quantitative experimental results have shown that Pd-coated surfaces become essentially opaque (i.e. $T_1 \rightarrow 0$) when the reflectivity $R_1 \sim 50\%$ [11]. For simplicity, the transmittivity of the Pd coating was thus assumed to be of the empirical form $T_1 = \exp(-9\mathrm{R}_1)$, which confirms to our experimental observations with the three Pd/PVDF/bare sensors. This relation has allowed a one-to-one correspondence between the effective reflectance and transmittance of the sensor and the reflectivity of the palladianized front surface. Since the effective transmittance T_{eff} is very sensitive to the reflectivity of the back surface R_2, Fig. 8(b) has been plotted with each curve normalized to its own first point ($R_1 = 0$), and can be called *normalized* effective transmittance, in order to show the dependence on R_1 for various R_2 values. From Fig. 8, we can see that R_{eff} is dominated by the reflectivity R_1 of the Pd coating in the region $R_1 \geq 0.2$ ("region 1"). This is due to

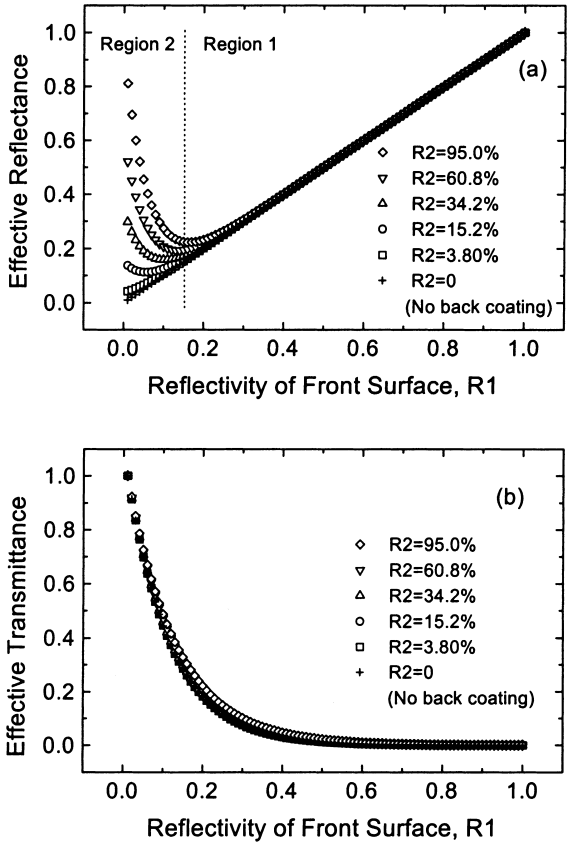

Fig. 8. Theoretical effective reflectance (a), and *normalized* effective transmittance (b) of a Pd/PVDF/NiAl hydrogen sensor as functions of the Pd-coated (front-surface) reflectivity for several back-surface-coating reflectivities.

the fact that the front surface is virtually opaque in region 1, and the contribution of the multiple internal reflections from the back coating is negligible. In region 2 ($R_1 < 0.2$), the effective reflectance becomes sensitive to the reflectivity of the back-surface coating. In the case of thin coatings (e.g. $R_2 < 3.8\%$), R_{eff} shows the same behavior as without any backing coating ($R_2 = 0$). Fig. 8(a) predicts that, if a sample with a thin (or no) back-surface coating is exposed to hydrogen gas, R_{eff} will decrease monotonically for all values of R_1, as observed experimentally. However, when the back-coating thickness increases, i.e. R_2 increases, R_{eff} will also increase as the Pd reflectivity decreases, because more incident light penetrates across the PVDF bulk and is strongly reflected by the backing metal coating, thus contributing to the overall reflectance of the sensor structure. This is clearly shown in Fig. 8(a) in the form of the appearance of a reflectance minimum for curves with $R_2 > 15\%$. The slopes of these curves with decreasing R_1 are found to be proportional to the reflectance of the back-surface coating. As shown in region 2 of Fig. 8(a), the increase in R_{eff} is greater for higher back-surface reflectivity R_2, especially as R_1 decreases toward zero. This can be seen in a semi-quantitative manner by comparing Fig. 4 with Fig. 5(a) and Fig. 6(a) with Fig. 6(b). For the same 6.5 nm Pd thickness (Figs. 4 and 5(a)), the reflectance change upon introduction of hydrogen was $\Delta R \sim 0.01$ mV before removal of the NiAl coating, while ΔR was only ~ 0.0024 mV after removing the NiAl coating. The same is true for Fig. 6(a) and (b), where $\Delta R \sim 0.003$ mV before NiAl coating removal, compared with $\sim$0.0005 mV after the removal of the back coating. As regards the transmitted signal, Fig. 8(b), it is seen that the *normalized* T_{eff} essentially exhibits insensitivity to the value of the reflectivity of the back-surface coating, and it increases with decreasing front-surface reflectivity, as observed in our experiments.

4. Conclusion

In this work, the reflectance inversion phenomenon observed in layered Pd/PVDF/NiAl hydrogen sensors with decreasing Pd-film thickness was studied methodically, including the effect of the back-surface coating on the measured optical reflectance signal. All the experimental results were found to be well-explained by means of a multiple-internal-reflection theoretical model. This theoretical explanation encompasses the Pd thickness range used by Kalli et al. [13]. In their case, the back-surface coating is actually the high-reflectivity crystalline Si substrate ($\sim$30%). In view of this configuration, Fig. 8(a) very likely covers the inversion phenomena reported by those authors. In addition, the steep increases in R_{eff} with increasing R_2 in region 2, would result in higher detectivity for a given hydrogen sensor device, when the system noise remains relatively constant. Therefore, the detectivity of an optical hydrogen sensor in the case of very thin Pd coatings (desirable for very fast response to the presence of ambient hydrogen gas [12]) can be enhanced by employing a highly reflecting coating on the back surface.

Acknowledgements

The support of the Natural Sciences and Engineering Research Council of Canada (NSERC) through an Operating Grant is gratefully acknowledged.

References

[1] A. Mandelis, C. Christofides, Physics, chemistry and technology of solid state gas sensor devices, in: J.D. Winefordner (Ed.), Chemical Analysis, Vol. 125, Wiley, New York, 1993.
[2] M.C. Steele, B.A. MacIver, Palladium/cadmium-sulfide Schottky diode for hydrogen detection, Appl. Phys. Lett. 28 (1976) 687–688.
[3] K.I. Lundstrom, M.S. Shivaraman, C.M. Svensson, A hydrogen-sensitive Pd-gate MOS transistor, J. Appl. Phys. 46 (1975) 3876–3881.
[4] A. D'Amico, A. Palma, E. Verona, Palladium-surface acoustic wave interaction for hydrogen detection, Appl. Phys. Lett. 41 (1982) 300–301.
[5] M.A. Butler, Fiber optic sensor for hydrogen concentrations near the explosive limit, J. Electrochem. Soc. 138 (1991) 46–47.
[6] M.A. Butler, Micromirror optical-fiber hydrogen sensor, Sens. Actuators B 22 (1994) 155–163.
[7] G. Fortunato, A. Bearzotti, C. Caliendo, A. D'Amico, Hydrogen sensitivity of Pd/SiO_2/Si structure: a correlation with the hydrogen-induced modifications on optical and transport properties of α-phase Pd films, Sens. Actuators 16 (1989) 43–54.
[8] B. Chadwick, J. Tann, M. Brungs, M. Gal, A hydrogen sensor based on optical generation of surface plasmons in a palladium alloy, Sens. Actuators B 17 (1994) 215–220.
[9] A. Mandelis, C. Christofides, Photopyroelectric (P^2E) sensor for trace hydrogen gas detection, Sens. Actuators B 2 (1990) 79–87.
[10] R. Wagner, A. Mandelis, Separation of thermal-wave and optical reflectance effects in palladium-photopyroelectric hydrogen sensors, Ferroelectrics 165 (1995) 193–203.
[11] A. Mandelis, J.A. Garcia, Pd/PVDF thin film hydrogen sensor based on laser-amplitude-modulated optical-transmittance: dependence on H_2 concentration and device physics, Sens. Actuators B 49 (1998) 258–267.
[12] C.H. Wang, A. Mandelis, J.A. Garcia, Detectivity comparison between thin-film Pd/PVDF photopyroelectric interferometric and optical reflectance hydrogen sensors, Rev. Sci. Instrum. 70 (1999) 4370–4376.
[13] K. Kalli, A. Othonos, C. Christofides, Temperature-induced reflectivity changes and activation of hydrogen sensitive optically thin palladium films on silicon oxide, Rev. Sci. Instrum. 69 (1998) 3331–3338.
[14] E.D. Palik, Handbook of Optical Constants of Solids, Academic Press, FL, 1985, p. 25.
[15] L. Ley, Photoemmision and optical properties, in: D. Joannopoulos, G. Lucovsky (Eds.), The Physics of Hydrogenated Amorphous Silicon II, Topics in Applied Physics, Vol. 56, Springer, Berlin, 1984, Chapter 3, 4, pp. 125–131.
[16] KYNAR Piezo Film Technical Manual, Pennwalt, King of Prussia, PA, 1983.